

SUPPORTING INFORMATION

About the importance of purge time in molecular layer deposition of alucone films

Hardik Jain^{a,b}, Paul Poodt^{a,b}*

^aTNO/Holst Centre, 5656 AE Eindhoven, Netherlands

^bDepartment of Applied Physics, Eindhoven University of Technology, 5600 MB Eindhoven, The Netherlands

(*paul.poodt@tno.nl)

Contents

A. Evaluating scaling laws for the outgassing TMA flux.....	S-2
A1. TMA exposure.....	S-3
A2. TMA purge step.....	S-4
Case I: Long TMA exposure times.....	S-4
Case II: Short TMA exposure times	S-6
B. Fitting results	S-12
C. Arrhenius plots of Γ_0 and τ_p	S-15
D. Experimental details for alucone films prepared using DMAI and EG.....	S-17
References	S-17

A. Evaluating scaling laws for the outgassing TMA flux

The MLD layer can be described as a plane sheet with a finite thickness between its two surfaces at $x = 0$ and $x = l$. The one-dimensional solution to the diffusion equation for this geometry is given by Crank¹.

For a TMA concentration at the two surfaces given by

$$C = C_1 \quad \text{at } x = 0 \text{ and } t \geq 0$$

$$C = C_2 \quad \text{at } x = l \text{ and } t \geq 0$$

and an initial concentration distribution within the sheet given by

$$C_0 = f(x') \quad \text{for } 0 < x' < l \text{ and } t = 0$$

the concentration distribution within the plane sheet is given by

$$C(x, t) = C_1 + (C_2 - C_1) \frac{x}{l} + \frac{2}{\pi} \sum_{n=1}^{\infty} \frac{C_2 \cos(n\pi) - C_1}{n} \sin\left(\frac{n\pi x}{l}\right) \exp\left(\frac{-D\pi^2 n^2 t}{l^2}\right) + \frac{2}{l} \sum_{n=1}^{\infty} \sin\left(\frac{n\pi x}{l}\right) \exp\left(\frac{-D\pi^2 n^2 t}{l^2}\right) \int_{x'=0}^l f(x') \sin\left(\frac{n\pi x'}{l}\right) dx' \quad (\text{S1})$$

with D the diffusion coefficient of TMA in the MLD film.

The interface between the MLD film and the substrate is impermeable for TMA, meaning that the concentration gradient at the interface is zero. This condition holds at the central plane of a sheet provided the initial and boundary conditions are symmetrical about that plane. This can be realized when taking $l = 2h$ with h the MLD film thickness. Solving Eqn. S1 for $x = 0$ to $x = l$ will then give a solution for the TMA concentration in the MLD film for $x = 0$ to $x = h$ which is consistent with all sorts of symmetrical boundary conditions.

A1. TMA exposure

To begin, we assume a simple case of an MLD film with thickness h and a zero initial TMA concentration throughout the film. The film is then exposed to a TMA partial pressure of P_{TMA} at its surface. If we assume a linear sorption isotherm, the relation between the partial pressure (P_{TMA}) and the TMA concentration at the film's top surface is given by $C = S P_{TMA}$, with S being TMA's solubility in the MLD film. In order to be able to use Eqn. S1 in this case, symmetrical boundary and initial conditions have to be employed where $C_1 = C_2 = S P_{TMA}$ and $C_0 = f(x') = 0$ respectively. The concentration distribution within the film after a TMA exposure time of $t = t_{TMA}$ is then given by:

$$C(x, t_{TMA}) = S P_{TMA} + \frac{2}{\pi} \sum_{n=1}^{\infty} \left(\frac{(S P_{TMA} \cos(n\pi) - S P_{TMA}) \sin\left(\frac{n\pi x}{l}\right) \exp\left(\frac{-Dn^2\pi^2 t_{TMA}}{l^2}\right)}{n} \right) \quad (S2)$$

As an example, Figure S1 shows the concentration profile in the MLD film for various exposure times, expressed as a function of the normalized distance $\left(\frac{x}{h}\right)$ from the film surface. For a TMA exposure time satisfying $\frac{D\pi^2 t_{TMA}}{h^2} < 1$, the TMA penetration depth is shallow and the concentration profile can be approximated by a complementary error function given by,

$$C(x, t_{TMA}) = C_0 \operatorname{erfc} \left[\frac{x}{2\sqrt{Dt_{TMA}}} \right] \quad (S3)$$

Where C_0 is the TMA concentration at the surface of the film.

Figure S1 also shows that the concentration distributions of TMA satisfying the condition $\frac{D\pi^2 t_{TMA}}{h^2} < 1$ can be fitted satisfactorily using Eqn. S3. For very long exposure times, the film

is completely filled with TMA and then the TMA concentration can be approximated as $C =$

$$C_{sat} = S P_{TMA}.$$

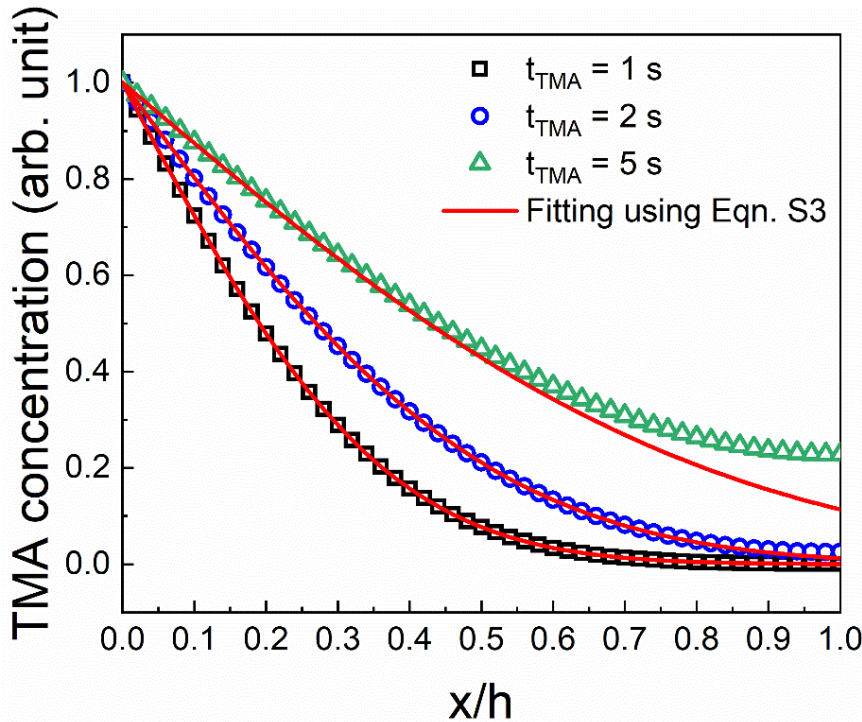


Figure S1: TMA concentration distribution within an MLD film evaluated for a range of exposure times t_{TMA} by numerically solving Eqn. S2 using a diffusion coefficient $D = 1 \times 10^{-18} \text{ m}^2/\text{s}$, $l = 10 \times 10^{-9} \text{ m}$, surface concentrations of $C_1 = C_2 = 1 \text{ arb. unit}$ and an initial uniform concentration of $C_0 = f(x') = 0$ within the film. For $\frac{D\pi^2 t_{TMA}}{h^2} < 1$, the concentration distribution can be approximated by using Eqn. S3.

A2. TMA purge step

During the TMA purge step, the boundary conditions for Eqn. S1 become $C_1 = C_2 = 0$. The initial concentration profile within the film $f(x')$ would understandably depend upon the previous exposure step.

Case I: Long TMA exposure times

In case the MLD film is saturated with TMA after the TMA exposure step (i.e. $\frac{D\pi^2 t_{TMA}}{h^2} \gg 1$),

the initial concentration profile can be approximated as $f(x) = C_{sat} = S P_{TMA}$. With these

boundary conditions, the concentration profile within the film after a TMA purge time of $t = t_p$ is given by

$$C(x, t_p) = \frac{2}{l} \sum_{n=1}^{\infty} - \left(\frac{l \sin\left(\frac{n\pi x}{l}\right) \exp\left(\frac{-Dn^2\pi^2 t_p}{l^2}\right) S P_{TMA}(\cos(n\pi) - 1)}{n\pi} \right) \quad (S4)$$

We are interested in the amount of TMA diffusing out of the film (i.e. the TMA flux j_{TMA} as a function of its purge time). The TMA flux at the film's surface is given by

$$j_{TMA} = D \left. \frac{dC(x, t_p)}{dx} \right|_{x=0} = \frac{2D}{l} \sum_{n=1}^{\infty} - \exp\left(\frac{-Dn^2\pi^2 t_p}{l^2}\right) S P_{TMA} (\cos(n\pi) - 1) \quad (S5)$$

The outgassing flux of TMA is plotted in Figure S2 as a function of its purge time expressed as $\frac{D\pi^2 t_p}{h^2}$. For short TMA purge times ($\frac{D\pi^2 t_p}{h^2} < 2$), the flux scales as $j_{TMA} \propto \frac{1}{\sqrt{t_p}}$ while for long

purge times ($\frac{D\pi^2 t_p}{h^2} > 2$), the flux scales as $j_{TMA} \propto \exp\left(-\frac{t_p}{\tau}\right)$, with τ being a time-constant.

It can also be seen from Eqn. S4 that, for both short and long purge times, the TMA flux scales as $j_{TMA} \propto P_{TMA}$.

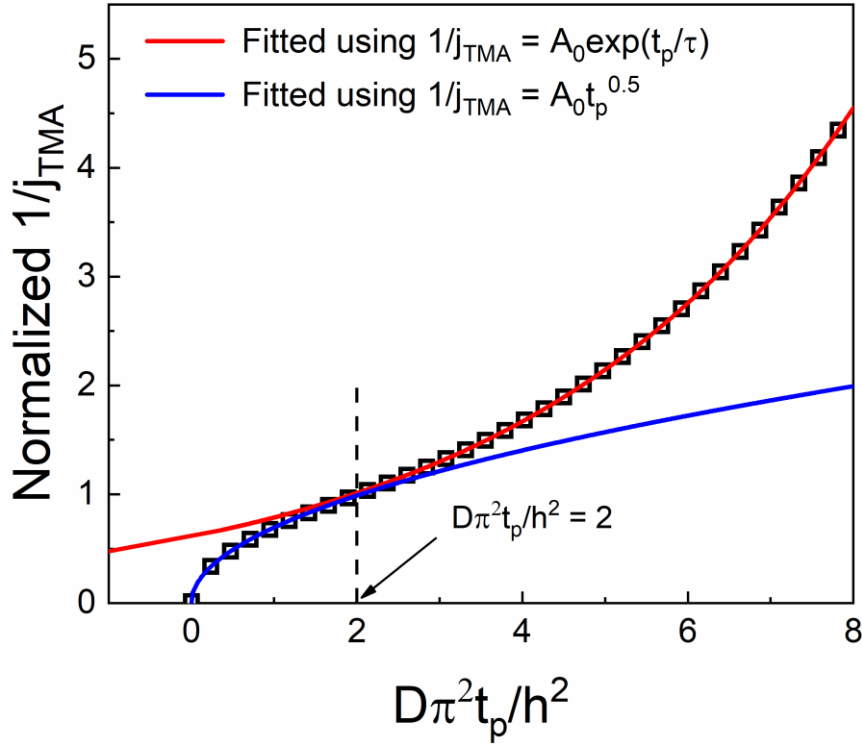


Figure S2: Variation of the outgassing TMA flux (expressed as $1/j_{TMA}$) from a saturated film ($C_0 = S P_{TMA}$) as a function of purge time (expressed as $\frac{D\pi^2 t_p}{h^2}$) evaluated using Eqn. S5. For small purge times ($\frac{D\pi^2 t_p}{h^2} < 2$), the flux decays as $1/\sqrt{t_p}$ whereas for long purge times ($\frac{D\pi^2 t_p}{h^2} > 2$), it decays as $\exp\left(-\frac{t_p}{\tau}\right)$.

Case II: Short TMA exposure times

For short TMA exposure times (i.e. $\frac{D\pi^2 t_{TMA}}{h^2} < 1$), the concentration profile inside the MLD film can be expressed as a complementary error function (see Eqn. S3 and Figure S1). To maintain symmetry around the $x = h$ plane as discussed before, the concentration profile after a given TMA exposure time (t_{TMA}) can be approximated using

$$C(x, t_{TMA}) = S P_{TMA} \left(\operatorname{erfc} \left[\frac{x}{2\sqrt{D t_{TMA}}} \right] + \operatorname{erf} \left[\frac{x-l}{2\sqrt{D t_{TMA}}} \right] + 1 \right) \quad (S6)$$

By substituting Eqn. S6 in Eqn. S1 for $f(x')$, we can calculate the TMA flux j_{TMA} which is given by

$$j_{TMA} = \frac{2D}{l} \sum_{n=1}^{\infty} \frac{n\pi \exp\left(\frac{-Dn^2\pi^2 t_p}{l^2}\right) S P_{TMA}}{l} \int_0^l \left(\operatorname{erfc}\left[\frac{x'}{2\sqrt{D t_{TMA}}}\right] + \operatorname{erf}\left[\frac{x' - l}{2\sqrt{D t_{TMA}}}\right] + 1 \right) \sin\left(\frac{n\pi x'}{l}\right) dx' \quad (S7)$$

For a given short exposure time of TMA satisfying $\left(\frac{D\pi^2 t_{TMA}}{h^2} < 1\right)$, Figure S3 shows the variation in the outgassing flux of TMA after a purge time (t_p) expressed as $\frac{D\pi^2 t_p}{h^2}$. For long purge times $\left(\frac{D\pi^2 t_p}{h^2} > 2\right)$, the TMA flux again scales as $j_{TMA} \propto \exp\left(-\frac{t_p}{\tau}\right)$, while for short purge times $\left(\frac{D\pi^2 t_p}{h^2} < 2\right)$, the flux does not scale as $j_{TMA} \propto \frac{1}{\sqrt{t_p}}$ but can be approximated by a summation of exponential terms i.e. $j_{TMA} \propto \sum_{n=1}^{\infty} A_n \exp\left(-\frac{t_p}{\tau_n}\right)$. The fit in Figure S3 inset was achieved using the first 3 terms of the summation i.e. $n = 1 \rightarrow 3$. Again it can be shown that, for both short and long purge times, the TMA flux scales as $j \propto P_{TMA}$.

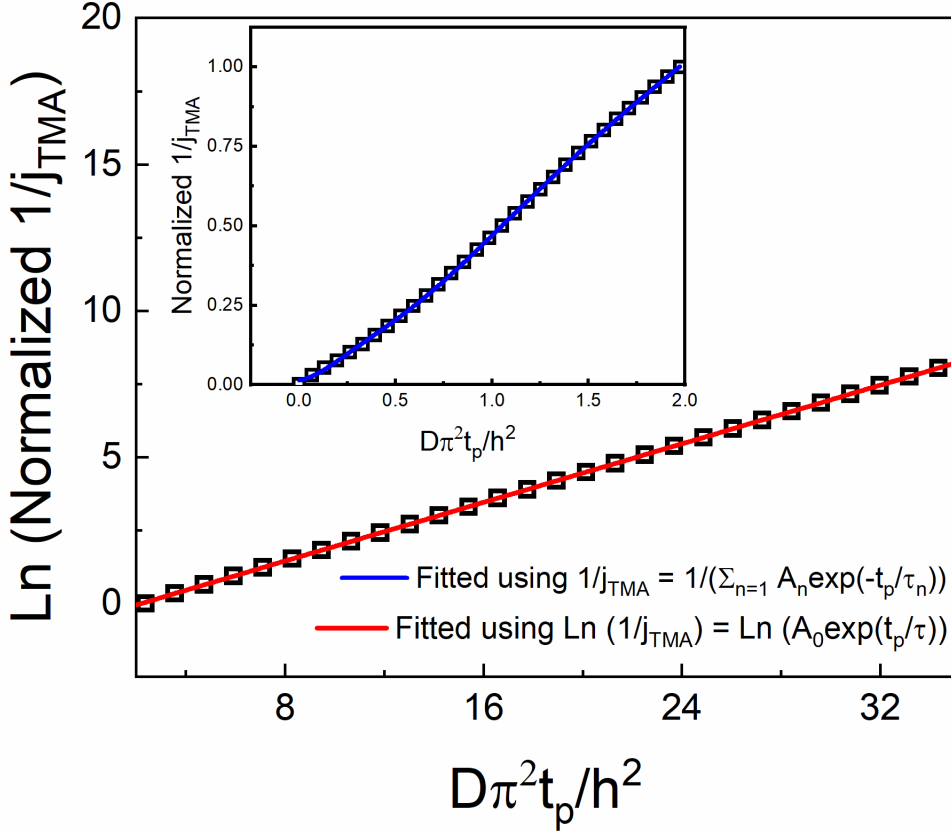


Figure S3: Variation of the outgassing TMA flux (expressed as $1/j_{TMA}$) as a function of purge time (expressed as $\frac{D\pi^2 t_p}{h^2}$) evaluated using Eqn. S7 for a short exposure time ($\frac{D\pi^2 t_{TMA}}{h^2} < 1$). For short purge times ($\frac{D\pi^2 t_p}{h^2} < 2$), the flux as shown in Figure S3 (inset) does not follow any scaling law but can only be approximated by a summation of exponential terms i.e. $j_{TMA} \propto \sum_{n=1}^{\infty} A_n \exp\left(-\frac{t_p}{\tau_n}\right)$ whereas for long purge times ($\frac{D\pi^2 t_p}{h^2} > 2$), the flux appears to decay as $\exp\left(-\frac{t_p}{\tau}\right)$.

It should be noted that for long purge times ($\frac{D\pi^2 t_p}{h^2} > 2$), the TMA flux j_{TMA} will also scale with the film thickness (h) whereas for short purge times ($\frac{D\pi^2 t_p}{h^2} < 2$), the flux becomes independent of the film's thickness after a film thick enough ($h > \sqrt{\frac{D\pi^2 t_p}{2}}$) has been grown.

For instance, starting with zero initial concentration within the film and fixed TMA exposure and purge times, we have iteratively solved Eqn. S7 for a range of film thicknesses and the

solution is plotted in Figure S4. It can be seen that only when $\frac{h^2}{D\pi^2 t_p} > \frac{1}{2}$ which corresponds to

$h > \sqrt{\frac{D\pi^2 t_p}{2}}$, the flux becomes constant and independent of the film thickness.

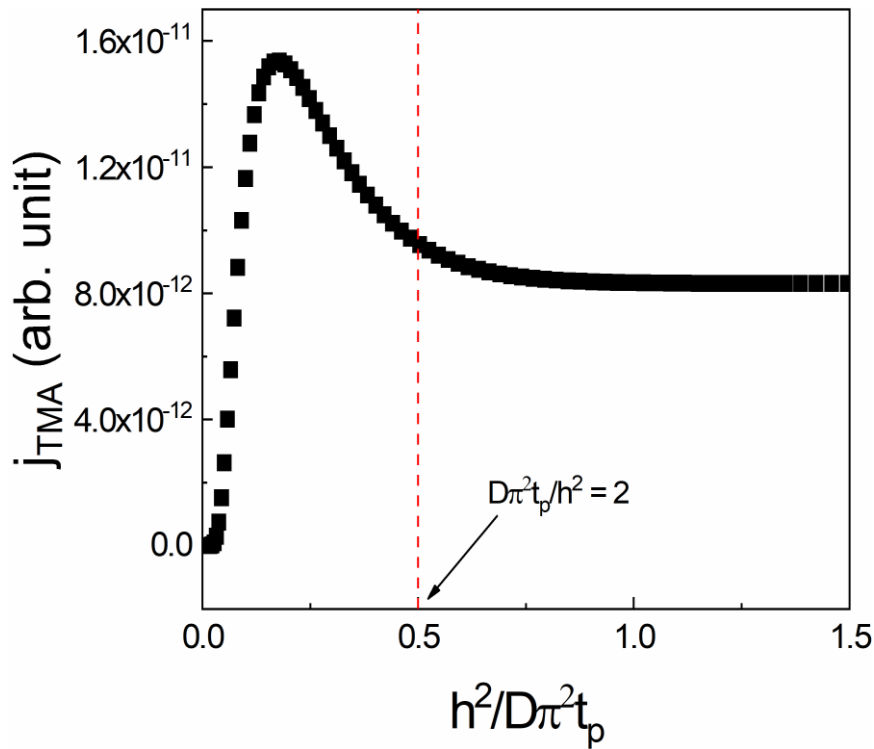


Figure S4: The outgassing TMA flux as a function of film's thickness expressed as $\frac{h^2}{D\pi^2 t_p}$. The flux becomes constant and independent of the film's thickness when $h > \sqrt{\frac{D\pi^2 t_p}{2}}$.

For a given purge time, in order to see the effect of TMA exposure time on the outgassing flux, we have solved Eqn. S7 for a range of short TMA exposure time ($\frac{D\pi^2 t_{TMA}}{h^2} < 1$). This has been separately done for a short ($\frac{D\pi^2 t_p}{h^2} < 2$) and a long ($\frac{D\pi^2 t_p}{h^2} > 2$) TMA purge time as shown in Figure S5. In both cases, it appears that the outgassing flux varies as $j_{TMA}(t_{TMA}) \propto 1 - \exp\left(-\frac{t_{TMA}}{\tau}\right)$ where τ is a time constant.

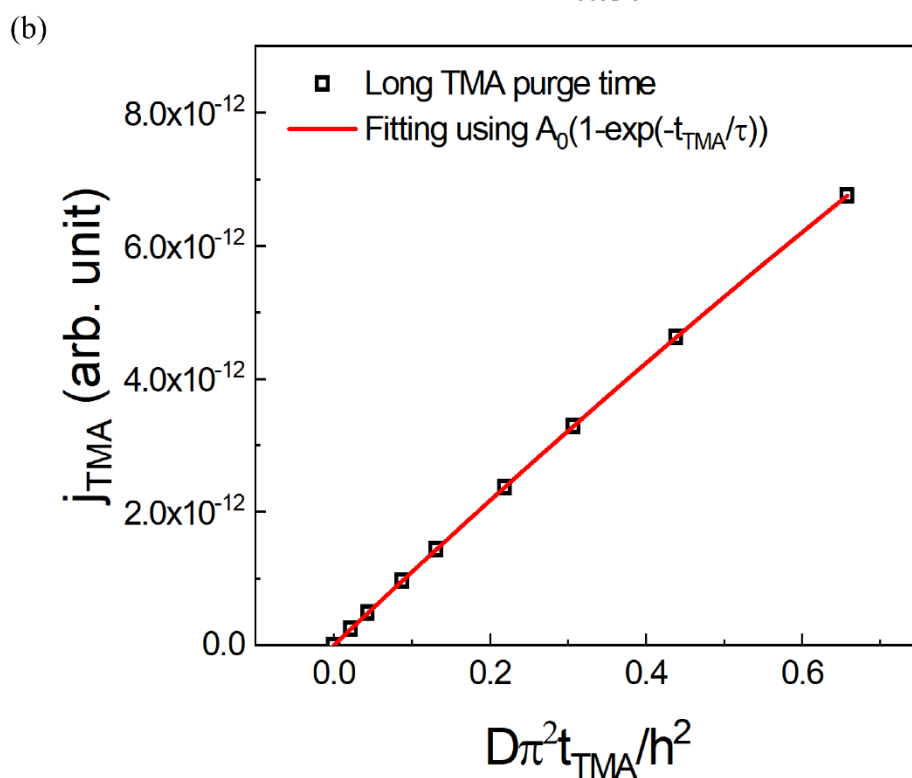
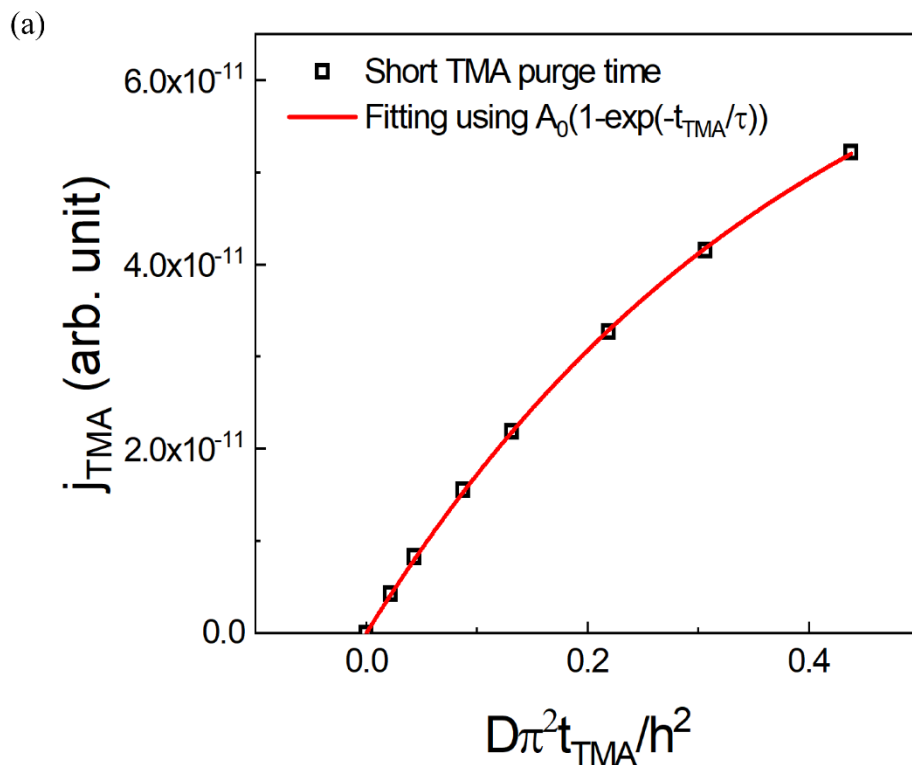


Figure S5: Variation of the outgassing TMA flux as a function of its exposure time evaluated using Eqn. S7 for short ($\frac{D\pi^2 t_p}{h^2} < 2$) and long ($\frac{D\pi^2 t_p}{h^2} > 2$) purge times. For short (S5-a) as well as long purge times (S5-b), the outgassing flux varies asymptotically with TMA's exposure time as $1 - \exp\left(-\frac{t_{TMA}}{\tau}\right)$.

Table S1 summarizes the scaling laws extracted from the plane sheet diffusion analysis. Further, from the experimental data, it can be concluded that we are in the short TMA exposure time – short purge time regime. Typical TMA exposure times we used are < 1 s, while the longest purge time tested was 98.4 s. The thinnest film deposited using 98.4 s as the purge time is around 20 nm thick. From this, we can estimate the order of magnitude of TMA's diffusion coefficient which is found to be smaller than 10^{-18} m²/s.

Table S1: Summary of the scaling laws derived for the outgassing TMA flux as a function of its partial pressure, exposure and purge times.

	Short TMA exposure time $\left(\frac{D\pi^2 t_{TMA}}{h^2} < 1\right)$	Long TMA exposure time $\left(\frac{D\pi^2 t_{TMA}}{h^2} > 1\right)$
Short TMA purge time $\left(\frac{D\pi^2 t_p}{h^2} < 2\right)$	$j \propto S P_{TMA}$ $j \propto 1 - \exp\left(-\frac{t_{TMA}}{\tau_e}\right)$ $j \propto \sum_{n=1}^{\infty} A_n \exp\left(-\frac{t_p}{\tau_{p,n}}\right)$	$j \propto S P_{TMA}$ $j \propto \frac{1}{\sqrt{t_p}}$
Long TMA purge time $\left(\frac{D\pi^2 t_p}{h^2} > 2\right)$	$j \propto S P_{TMA}$ $j \propto 1 - \exp\left(-\frac{t_{TMA}}{\tau_e}\right)$ $j \propto \exp\left(-\frac{t_p}{\tau_p}\right)$	$j \propto S P_{TMA}$ $j \propto \exp\left(-\frac{t_p}{\tau_p}\right)$

B. Fitting results

The experimentally observed variations of Γ_{Total} as a function of TMA purge time as shown in Figure 4 of the publication were fitted with Eqn. 12 of the publication. The fitting was performed in OriginPro 2018 using a Levenberg Marquardt iteration method. The fitting results for each partial pressure of TMA are shown in Figure S6.

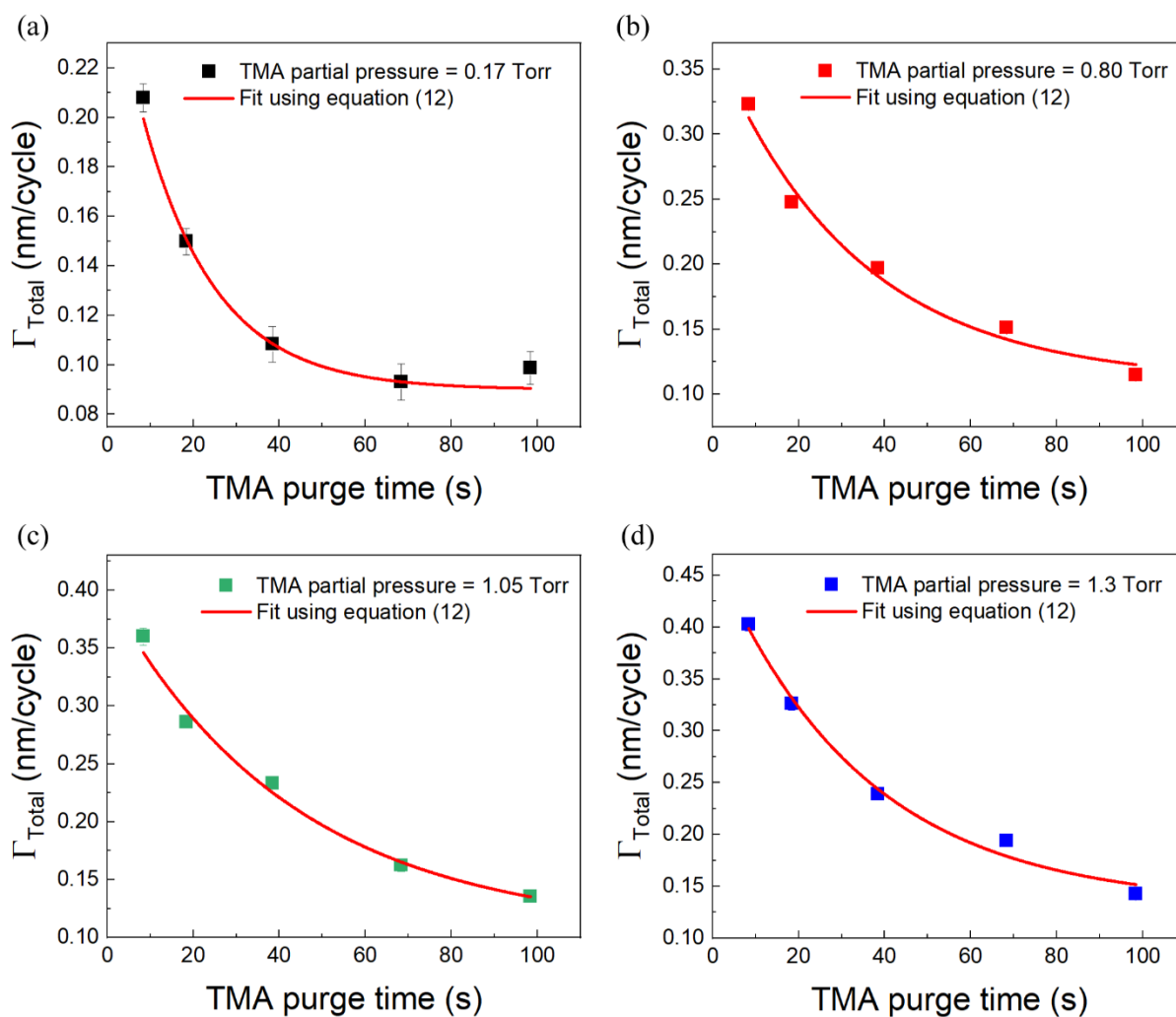


Figure S6: Fitting of the data in Figure 4 of the publication with Eqn. 12 of the publication. a) TMA partial pressure = 0.17 Torr; b) TMA partial pressure = 0.80 Torr; c) TMA partial pressure = 1.05 Torr; d) TMA partial pressure = 1.3 Torr.

Table S2 summarizes the extracted values of model parameters and the respective standard errors from fitting.

Table S2: Extracted values of the model parameters at different TMA partial pressures

Figure	TMA partial pressure (Torr)	Γ_{MLD} (nm/cycle)	Γ_0 (nm/cycle)	$\frac{\tau_p}{a}$ (s)	Reduced χ^2
S6-a	0.17	0.09 ± 0.01	0.18 ± 0.03	17 ± 4	1.9
S6-b	0.80	0.11 ± 0.03	0.26 ± 0.03	33 ± 11	14.3
S6-c	1.05	0.11 ± 0.02	0.29 ± 0.02	43 ± 10	5.8
S6-d	1.33	0.13 ± 0.02	0.34 ± 0.02	35 ± 9	6.3

Similarly, the experimentally observed variations of Γ_{Total} with TMA purge time for different deposition temperatures as shown in Figure 6 of the publication were also fitted with Eqn. 12 of the publication. The fitting results for each deposition temperature are shown below in Figure S7. The extracted values of the model parameters are displayed in Table S3.

Table S3: Extracted values of the model parameters at different deposition temperatures

Figure	Deposition temperature ($^{\circ}\text{C}/\text{K}$)	Γ_{MLD} (nm/cycle)	Γ_0 (nm/cycle)	τ_p (s)	Reduced χ^2
S7-a	100/373	0.30 ± 0.01	0.39 ± 0.05	9 ± 2	2.2
S7-b	125/398	0.23 ± 0.03	0.33 ± 0.03	13 ± 5	12.3
S7-c	150/423	0.11 ± 0.02	0.29 ± 0.02	16 ± 4	5.8

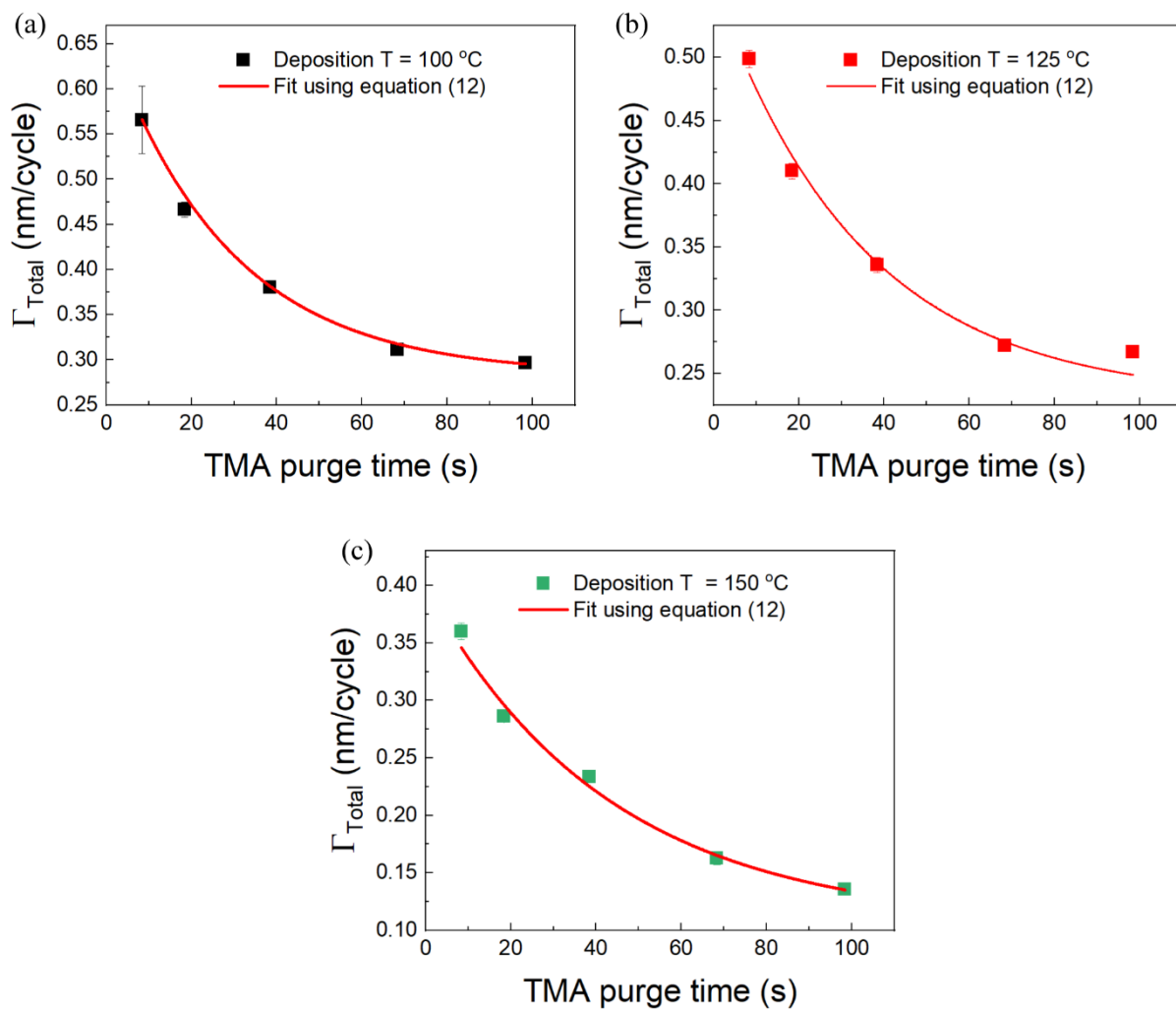


Figure S7: Fitting the data in Figure 6 of the publication with Eqn. 12 of the publication. a) Deposition temperature = 100 °C; b) Deposition temperature = 125 °C; c) Deposition temperature = 150 °C

C. Arrhenius plots of Γ_0 and τ_p

The temperature dependence of model parameters Γ_0 and τ_p can be described by an Arrhenius relation. The general form of an Arrhenius relation is given by,

$$A = A_0 \exp\left(\frac{-E_a}{RT}\right) \quad (\text{S8})$$

Where,

A_0 = Pre-exponent factor

E_a = Activation energy (J mol^{-1})

R = Gas constant ($\text{J K}^{-1} \text{mol}^{-1}$)

T = Absolute temperature (K)

Figure S8 shows Arrhenius plots of $\ln \Gamma_0$ (a) and $\ln \tau_p$ (b). Linear regressions of both plots reveal the values of corresponding activation energies and pre-exponent factors. These are shown in Table S4.

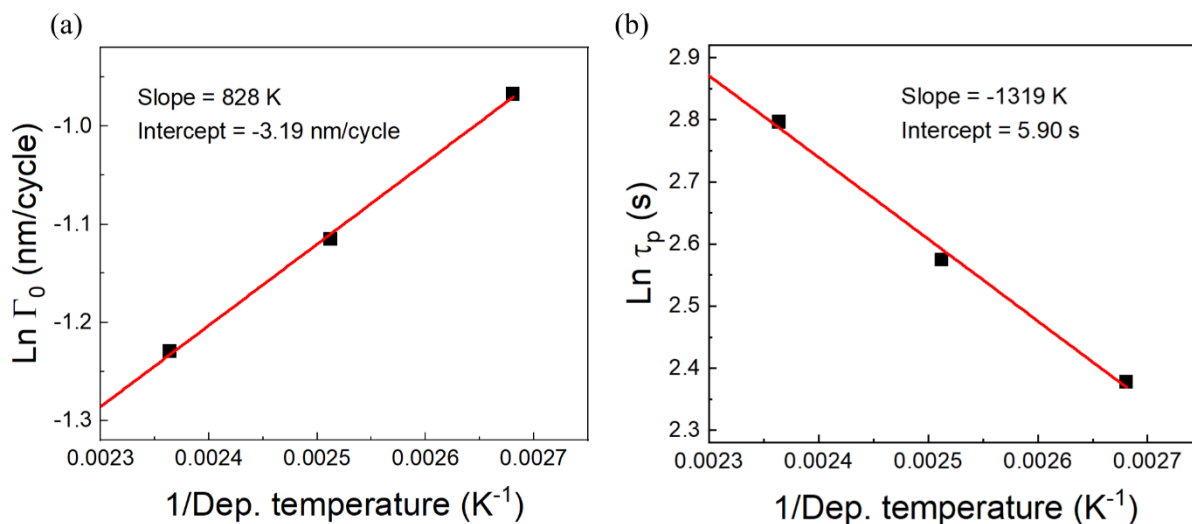


Figure S8: Arrhenius plots of model parameters a) Γ_0 b) τ_p .

Table S4: Extracted values of activation energies and pre-exponent factors for Γ_0 and τ_p .

Plot	E_a (kJ/mol)	Pre-exponent factor	Residual sum of squares
$\ln \Gamma_0$ vs. $1/T$	-6.88 ± 0.25	-3.19 ± 0.08 (nm/cycle)	4.83×10^{-4}
$\ln \tau_p$ vs. $1/T$	10.97 ± 0.8	5.90 ± 0.24 (s)	4.51×10^{-4}

D. Experimental details for alucone films prepared using DMAI and EG

Dimethylaluminum isopropoxide (DMAI) from Strem Chemicals, Inc. and ethylene glycol (EG) from Sigma Aldrich (99.8 %) were used as reactants. Both the reactants were dosed using a bubbler assembly. In order to increase the vapor pressure of the reactants, ethylene glycol bubbler was heated to 100 °C while dimethylaluminum isopropoxide bubbler was heated to 75 °C. Partial pressures of the reactants were set by adjusting the carrier and dilution flows. The total volumetric flow (carrier + dilution flows) for each reactant was kept constant at 0.4 slm. All depositions were carried out at 150 °C. Double-sided polished Si wafers of diameter 150 mm and a thickness of 0.7 mm were used as substrates. The thicknesses of the films were measured within 15 mins of their deposition using an ex-situ Horiba Jobin Yvon spectroscopic ellipsometer.

References

- 1 J. Crank, *The Mathematics of Diffusion*, CLARENDON PRESS, OXFORD, 1975.